REPORT DOCUMENTATION PAGE

Form Approved
OMB No. 0704-0188

1. AGENCY USE ONLY (Leave blank)	2. REPORT DATE	3. REPORT TYPE AND DATES COVERED
		FINAL 01 Sep 93 To 31 Aug 96

4. TITLE AND SUBTITLE

INTEGRATED OPTICAL POLYMER DEVICES

5. FUNDING NUMBERS

F49620-93-1-0557
61103D
3484/XS

6. AUTHOR(S)

Dr Anthony F. Garito

AFOSR-TR-97
0133

7. PERFORMING ORGANIZATION NAME(S) AND ADDRESS(ES)

Dept of Physics
Univ of Pennsylvania
209 South 33rd Street
Philadelphia PA 19104-6396

9. SPONSORING / MONITORING AGENCY NAME(S) AND ADDRESS(ES)

AFOSR/NL
110 Duncan Ave Room B115
Bolling AFB DC 20332-8080

Dr Charles Y-C. Lee

10. SPONSORING / MONITORING AGENCY REPORT NUMBER

11. SUPPLEMENTARY NOTES

12a. DISTRIBUTION / AVAILABILITY STATEMENT

[illegible] release;
[illegible].

12b. DISTRIBUTION CODE

13. ABSTRACT (Maximum 200 words)

Nonlinear optical processes in #-electron organic and polymer systems have attracted considerable interest because their understanding had led not only to complelling technological promise but also to new phenomena, new theoretical insights, and new materials and devices. The #-electron excitations occurring on the individual molecular, or polymer chain, units are the basic origin of the observed nonresonant nonlinear optical coefficients which are oftentimes unusally large. The coefficients are broad band and ultrafast, and, as shown by theory and experiment, their sign, magnitude and frequency dependence are determined by many-body electron correlation effects. This level of understand, in turn, now makes viable computer aided molecular design of new nonlinear optical chromophores.

19970314 054

14. SUBJECT TERMS

15. NUMBER OF PAGES

16. PRICE CODE

17. SECURITY CLASSIFICATION OF REPORT	18. SECURITY CLASSIFICATION OF THIS PAGE	19. SECURITY CLASSIFICATION OF ABSTRACT	20. LIMITATION OF ABSTRACT
(U)	(U)	(U)	(U)

FINAL REPORT

~~01 Jun 93-31 May 95~~

INTEGRATED OPTICAL POLYMER DEVICES

Grant Number: F49620-93-1-0557

PRINCIPAL INVESTIGATOR: Professor Anthony F. Garito (215) 898-5810

PROGRAM MANGER: Dr. Charles Lee (202) 767-4960

University of Pennsylvania
209 South 33rd Street
Philadelphia, PA 19104

Nonlinear Optics of Organic and Polymer Materials

A.F. Garito, R.F. Shi, and M.H. Wu

Department of Physics

University of Pennsylvania

Philadelphia, PA 19104

I. INTRODUCTION

Nonlinear optical processes in π-electron organic and polymer systems have attracted considerable interest because their understanding has led not only to compelling technological promise but also to new phenomena, new theoretical insights, and new materials and devices. The π-electron excitations occurring on the individual molecular, or polymer chain, units are the basic origin of the observed nonresonant nonlinear optical coefficients which are oftentimes unusually large. The coefficients are broad band and ultrafast, and, as shown by theory and experiment, their sign, magnitude and frequency dependence are determined by many-body electron correlation effects. This level of understanding, in turn, now makes viable computer aided molecular design of new nonlinear optical chromophores.

In recent years as the field has naturally progressed toward technological applications, the main issues have focused on high performance materials that comply with device manufacturing and end-use conditions. New challenges in materials synthesis are being presented, resulting in new methods of ultra structure synthesis and the discovery of entirely new materials and high performance compositions exhibiting high thermal, mechanical, and chemical stability. At the same time, there is increasing appreciation of the low cost, practical materials processing associated with these materials, especially polymer thin films and fibers. These include ease and flexibility in synthesis modification and formulation; film deposition by spin coating, spraying, or dipping; and ease in fiber fabrication.

It has now been demonstrated at pilot plant scales that high performance electrooptic polymer thin films can be routinely used in optoelectronic integrated circuit (OEIC) fabrication in existing microelectronic device manufacturing facilities. The key steps are standard, including spin coating, photolithography, etching, metallization, and multilayer

assembly. High optical quality polymer optical fibers (POF) have long been available commercially for their linear optical properties, and the wide spread use of optical grade polymers in ophthalmic lenses, compact discs, and laser discs is well established.

As the field continues its rapid acceleration, fortunately, there are valuable conference proceedings and comprehensive books published on these latest developments, especially within the last three years [1-6].

The nonlinear optical mechanisms in π-electron conjugated organic materials differ fundamentally from that of other materials because the nonlinear optical responses primarily originate from π-electron excitations on individual microscopic molecular or polymer chain units. In organic systems, on-site intramolecular π-electron interactions are orders of magnitude stronger than the relatively weak off-site intermolecular Van der Waals interactions between individual molecular or polymer chain units. Each unit can therefore be viewed as essentially an independent source of nonlinear optical response. The response of a macroscopic condensed assembly as in a solid can be calculated by simply summing the response of the individual molecular, or polymer chain, sites averaged over their orientations. This is in contrast to inorganic materials in which the optical responses arise from collective band structure effects.

The nonlinear optical properties of organic molecules are due to the character of their π electron systems. There are two types of bonds formed between atoms in organic molecules, σ bonds and π bonds. σ bonds between atoms result from the overlap of hybrid electron orbitals along the inter atomic axis. Electrons involved in σ bonds are tightly bound to their original atomic sites and thus are not greatly affected by the applied field. π bonds are typically formed from two π type orbitals which overlap above and below the molecular plane. π electrons (those involved in π bonds) are more loosely bound to the atomic nuclei than σ electrons, and thus are more easily polarizable. In molecules with alternating single and double bonds (known as conjugated molecules), π orbitals can

overlap along the entire length of the molecule, allowing the π electrons to move from one end of the molecule to the other. π electron systems in a conjugated system are easily and quickly polarizable by an applied optical electric field. The associated large redistribution of π electrons results in unusually large nonlinear optical responses.

The nonlinear optical responses of an organic and polymeric systems must be treated in the quantum regime and may be represented in either first, or second, quantization formalism. In each case, the input fields are treated as perturbations to the π-electrons. The molecular nonlinear optical coefficients $\beta_{ijk}(-\omega_3; \omega_1, \omega_2)$ and $\gamma_{ijkl}(-\omega_4; \omega_1, \omega_2, \omega_3)$ govern second and third order optical processes, respectively. They can then be individually described in terms of a basis set of eigenstates and eigenfunctions of the unperturbed system via time dependent perturbation theory. Usually, only the states due to excitation of π electrons are needed in these calculations. The expressions for the β and γ obtained through this process contain products of transition moments between states of the unperturbed system. These terms describe virtual transition sequences which prove critical to understanding the origin and mechanism of β and γ.

Analysis of the transition sequences which account for large fractions of the total coefficients has shown researchers which excited states are vital to the nonlinear optical processes. Study of the detailed nature of these π-electron excited states has, in turn, led to a more complete understanding of the nonlinear optical properties of organic and polymeric materials.

II. SECOND-ORDER OPTICAL PROCESSES IN ORGANIC MATERIALS

A. Microscopic Descriptions

Organic molecular and polymer chain structures possessing a π-electron system usually form symmetrically about a center point into so called centrosymmetric structures. As a result, these materials generally do not exhibit second order nonlinear optical effects.

The central symmetry point called an inversion center can be removed and the overall structural symmetry lowered to a noncentrosymmetric form by asymmetrically distorting the π-electron system. This is usually accomplished by chemically attaching electron donor and acceptor groups in diametrically opposed positions in the structure. This substitution is molecular analogue to *p* and *n*-type dopings in semiconductors. In Figure 1, the recently developed high thermal stability polyimide-like chromophore[7] serves as a timely example. The ten carbon site central π-electron rings (naphthalene rings) are substituted on the right by the amine (NH_2) containing donor group and oppositely on the left by the imide acceptor group. The resultant molecular ground state dipole moment points nearly uniaxially across the central rings from right to left–from the donor to acceptor regions of the chromophore.

The microscopic coefficient β is accurately described by quantum many-electron theory that explicitly accounts for electron correlation effects due to electron-electron Coulomb repulsions[8]. The motion of any one π-electron is not independent and free but dependent on the motion of all the other π-electrons. For many structures, theoretical calculations reveal that large values of β result from highly asymmetric, charge-correlated excited states. In particular, upon virtual excitations, electrons are removed from one end of the molecule to the other end along the molecular dipolar axis. A representative topographical contour map of the redistribution of π-electron density accompanying such an excitation to the first many-electron excited state for the case of newly developed high temperature chromophores is also shown in Figure 1. Electron density in the vicinity of the electron donor amino group on the right is transferred to the region of the electron acceptor on the left, resulting in a large charge separation and associated large optical transition moment. These diagrams clearly illustrate the microscopic origin and mechanism for second order optical responses in π-electron systems.

The ability to understand the basic physical mechanisms and thereby provide accurate microscopic descriptions of nonlinear optical processes has naturally enabled the

development of highly efficient supercomputer software code with which researchers are now able to accurately describe the nonlinear optical properties of a wide variety of π-electron structures. Calculations also reveal that in order to quantitatively predict the β response of a π-electron structure, high-lying correlated excited states are essential. Nevertheless, the most dominant contribution comes from the first excited state. Qualitatively or semi-quantitatively, three key parameters determine the second-order optical responses: the transition energy, the dipole moment difference and the transition moment between the excited (usually the first) and ground states. To enhance β, one has to decrease the first and increase the rest two parameters. A typical method to achieve this is to increase the electron donating and accepting strengths of the two side substituents (D and A) for the D-π-A type of molecules by using stronger donors and acceptors as well as to increase the conjugation length of the π bridge[9]. This can be done because strong donor and acceptors increase the charge transfer nature of the excited state, thereby enhancing the second-order optical responses. One interesting idea stemming out of this proposed recently by researchers at Caltech[10] is that one can tune β values of a system by using different solvents with different polarities to change the charge transfer nature of the ground and excited states. In this manner, one can maximize β or even change its sign.

The standard technique to measure the molecular susceptibility β in gases and liquid solutions is dc-induced-second-harmonic-generation [8][11][12] (DCSHG, or EFISH). A DC electric field applied across the sample aligns the dipolar molecules[13] to break the natural centrosymmetry. Numerous dipolar structures have been studied using DCSHG (EFISH) over the past decade. However, the technique is limited to dipolar molecules. Recently, Belgian researchers have developed the hyper-Rayleigh scattering (HRS) technique[14] of Maker and Terhune to overcome the limitations of the DCSHG (EFISH) method. In this technique, one measures the incoherent second harmonic scattered light from a solution with no necessity of applying a DC field. The new HRS method has been broadly applied to many systems that include not only dipolar molecules but ionic

materials[15], octupolar molecules[16][17], polymers, and proteins[18] which cannot be measured by DCSHG (EFISH).

Construction of bulk materials having large macroscopic $\chi^{(2)}$ requires not only molecular constituents with large microscopic β but also a noncentrosymmetric system where the orientation of the molecular species, best described by orientational distribution functions, results in constructive additivity of the molecular responses. In addition to standard crystal growth , approaches include electric field poling of amorphous polymer films (see Figure 2[19][20]), Langmuir-Blodgett films[21][22] (LBF), and molecular self-assembly[23-25]. The electric field poling approach[26-29] is particularly important due to the ease of film processing, multilayer capability, and compatibility with standard semiconductor manufacturing steps. In this approach, A DC electric field is applied across the polymer film sample that is heated to above its glass transition temperature to allow the dipolar chromophores to align with the field. The temperature is then lowered to the glass transition temperature to lock in the noncentrosymmetric orientational order. The intrinsic thermal relaxation, which could eventually destroy the noncentrosymmetry, can be greatly reduced in polymer systems with high glass transition temperatures. One elegant example is polyimide systems with glass transition temperatures greater than 360°C[30] that are currently one of the central focuses under intensive studies.

B. Linear Electrooptic (EO) Effects

The first applications of organic materials will likely be based on the EO properties of glassy polymers in integrated optic devices[31-33]. The linear electrooptic effect (also called Pockels effect), which belongs to second order optical processes with one input frequency being zero or very low, provides a means for changing the refractive index of a material by application of a dc, or low frequency, electric field. With an appropriate integrated optic device, the output optical field, modulated by the electric field, carries the

information of the electric field and can be decoded again after traveling long distances. The large EO coefficients combined with low dielectric constants in organic materials lead to comparative quantities, or figures of merit, for organic materials that far exceed traditional inorganic materials such as lithium niobate ($LiNbO_3$) and gallium arsenide (GaAs). The figure of merit is defined as the product of the cube of the refractive index and the EO coefficient divided by the dielectric constant. The materials comparison is illustrated in Figure 3. In addition, the operation bandwidth of an integrated optic device is limited by the velocity mismatch between the optical wave and microwave. This in turn is determined by the difference between the square root of the effective dielectric constant ($\sqrt{\varepsilon}$) and the effective refractive index (n) of the optical waveguide. The nearly vanishing mismatch between these two quantities in organic materials makes them excellent candidates for waveguiding materials in active, high speed integrated optic device applications.

As we stated earlier, the major obstacle to development of practical integrated optic devices using poled polymers is the thermal stability of the EO coefficients. Initial research efforts often involved polymethyl methacrylate (PMMA), whose low glass transition temperature leads to a loss of macroscopic alignment and a resulting decrease in the EO coefficient at expected device operating temperatures. Recent research has shown that polyimides[30][34][35], which are well known in the microelectronics industry for their ease of processing, low thermal expansion coefficients and their chemical stabilities at high temperatures, can be developed to act as both passive waveguides and as hosts for EO chromophores in active regions of devices. The focus of current research is now towards finding new chromophores that can withstand the stringent thermal and chemical stability conditions required in polyimide-based fabrication processes and device assembly steps. Recently, two major developments of new EO chromophores[7][36][37] have been reported. One involves a new class of high thermal stability, large second-order nonlinearity fused-ring EO chromophores, 1,8-naphthoylene-benzimidazoles[7] with one example having been shown in Figure 1, designed for their structural similarity to polyimide repeat units and

consequent easy incorporation into host polyimides. The other is related to donor-acceptor substituted heteroaromatic chromophores[37] that have exceptionally large second-order nonlinearities and good thermal stabilities. These new high thermal stability chromophores are the first realization of high EO coefficient guest molecules to qualify under real semiconductor fabrication conditions, thereby representing a critical step in the progress toward a true optical device technology.

The unique opportunity presented by high thermal stability EO polymer materials is the ability to design, build, and test novel integrated EO devices of unprecedented performance utilizing standard semiconductor device fabrication lines. Earlier, high density waveguide arrays for optical data processing were demonstrated in polyimide films using reactive ion ethching. An excellent perfect shuffle waveguide circuit is shown in Figure 4. Various EO modulation and waveguide coupling mechanisms are being developed and tested on active EO polymer modulators[38][39]. The purpose is to achieve high bandwidth performance as well as to minimize the voltage length product for future device integrations. In a simple Mach-Zehnder EO modulator, the applied field causes the refractive index in each arm to be different, resulting in a phase difference between the optical guided waves that is directly proportional to the EO figure of merit. Recently, researchers have also demonstrated an impressive high EO modulation of 40 GHz[40] driven by relatively low integrated circuit (IC) level voltages using materials similar to those of Figure 2. These results illustrate the great potential of EO polymers in high speed device applications.

C. Second Harmonic Generation

Optical frequency synthesis such as second harmonic generation (SHG), or frequency doubling, is an additional area of intense research on second order optical properties. Efficient SHG must meet not only the same requirements as efficient EO modulation but also additional ones associated with the coherent nature of the process[41].

For maximum SHG the material must possess propagation directions where the material birefringence cancels the natural optical dispersion, leading to the condition of equal refractive indices at the fundamental and second harmonic frequencies. This condition, known as phase matching, results in a high percentage of conversion of the input light to the output SHG. The SHG figure of merit is defined as the square of the SHG coefficient divided by the cube of the of the refractive index. The fact that low index values (1.3-1.8) characterize organic materials is a distinct advantage over the relatively large inorganic values (2.0-2.5).

Various approaches have been taken to take advantage of the ease of processing properties of organic materials to achieve phase matching conditions. They include single crystal-core fibers[42], where the molten organic is drawn by capillary action into a hollow core glass tube, free standing periodically stacked polymer films, where layers are alternately poled in opposite directions to achieve quasi phase matching conditions[43] and to form periodic "synthetic crystals" for through the plane applications, and organic waveguides using two Langmuir-Blodgett deposited films[44], in which precise control of the film thickness, together with inversion of $\chi^{(2)}$ across the film, are used to simultaneously achieve phase matching and improve the optical field overlap between the propagating waveguide modes. In each case, the second harmonic output efficiency is greatly enhanced.

Currently, SHG applications are centered on frequency doubling laser diode sources operating in the 800 nm range to the blue spectral region near 400 nm[45]. In optical data storage applications, the shorter wavelengths enable higher packing densities of optical data bits to be recorded and read. The issue associated with blue or violet light generation is the transparency of the material to the light. Most materials with high SHG efficiency show significant absorption in the blue or violet spectral region. Researchers have demonstrated tunabilty of SHG light using organic single crystals, as illustrated by the

dispersion results for MNA SHG coefficient in Figure 5, and have used these results as a basis for developing blue light sources using SHG.

III. THIRD-ORDER OPTICAL PROCESSES IN ORGANIC MATERIALS

A. Microscopic Descriptions

As we stated earlier, third-order optical effects $\chi^{(3)}$ are possible for all kinds of structures[46]; there are no symmetry restrictions on molecules as in the case of second-order optical processes. For organic and conjugated systems, it is found that the relatively large, ultrafast[47][48], nonresonant $\chi^{(3)}$ is due to the collective motion and electron-electron correlation effects of the π electrons that are delocalized over the entire molecule. The independent particle model, which neglects collective effects, is futile in determining the $\chi^{(3)}$ responses. The proper inclusion of the correlation effects, on the other hand, correctly predict the $\chi^{(3)}$ responses in terms of the sign, magnitude, and dispersion[49-54].

The physical origin of the microscopic third-order optical responses γ is made most clearly in centrosymmetric molecules where the electronic states have definite parities. These electronic states can be labeled as one-photon states which have different parities than the ground state, and two-photon states which have the same parity as the ground state. Quantum many-electron sum-over-states calculations show that there are usually two types of virtual transition sequences that dominate γ. The first type only involves the ground state (S_0) and certain one-photon state (S_1, normally the first excited one-photon state), in the form of $S_0 \rightarrow S_1 \rightarrow S_0 \rightarrow S_1 \rightarrow S_0$. This type contributes negatively to the total γ. The second type involves S_0, S_1 and some energetically high-lying two-photon state (S_2), in the form of $S_0 \rightarrow S_1 \rightarrow S_2 \rightarrow S_1 \rightarrow S_0$. This type contributes positively to the total γ. It is the strong competition between these two types that determines the sign and magnitude of γ. In both cases, the one-photon state acts as a gateway state that couples to the excited state

manifold. Furthermore, in most systems, due to the correlated motion, there is a large charge redistribution when electrons are excited to the two-photon state from the one-photon state, resulting in a large transition moment between these two states and a positive, nonresonant γ. Recently however, organic dyes having negative, nonresonant γ have been discovered[55]. It is found that in these dyes, the first type virtual transition sequence outweighs the second type, although the high-lying two-photon states are still critically important[56].

The quantum many-electron calculations that explicitly take into account electron-electron correlation effects are remarkably successful on small molecules where the number of π electrons is limited. For large molecules[50][57], because of the limited computation capability, the results are more qualitative than quantitative. However, for certain polymeric structures[58-60], the understanding of the behavior of the repeat units enables us to grasp the feature of the polymers as well. Figure 6 clearly demonstrates this where the third harmonic γ values[61] over a wide range of input photon energies are compared between theory and experiment for a prototype structure, poly-4BCMU.

Due to the collective, correlated motion of the π electrons, the γ value increases supralinearly as a function of the length L of the molecule. Figure 7[62] shows a log-log plot of $\gamma_{xxxx}(-3\omega;\omega,\omega,\omega)$ versus polyene chain length. The good linear fit indicates that possesses $\gamma_{xxxx}(-3\omega;\omega,\omega,\omega)$ a power law dependence on L with an exponent of 3.5. The strong dependence of γ on L is the primary reason for the intensive study in conjugated linear chains as nonlinear optical materials. The apparent similarity in power law behavior simply reflects the delocalized nature of the conjugated bonds in polyenes as compared to, for example, the linear dependence resulting from the bond additivity rule for localized bonds. As the chain length becomes longer, π electrons on one end of the molecule do not correlate those on the other end, resulting in the saturation of γ on L. The onset of saturation determines the correlation length of a conjugated system beyond which γ starts

increasing linearly with L. Figure 8 shows the phenomenon in oligothiophenes[63] in which the saturation behavior was first observed. It is concluded that the large, nonresonant values of γ, and correspondingly $\chi^{(3)}$, may require chains of only intermediate length, with little to be gained beyond certain limit. This is also the reason why novel materials and new physical understanding are needed before major applications of $\chi^{(3)}$ materials[64] become a reality.

As an example of our understanding of third-order optical effects in organic and conjugated structures, we can turn to C_{60}, buckminsterfullerene that has been received wide attention recently, including various nonlinear optical studies[65][66]. In this novel material, each molecule consists of 60 carbon atoms which possess single-bond/double-bond alternations. Although being like a three-dimensional soccer ball in structure, C_{60} is much different from one-dimensional structures such as polyenes, its nonlinear optical properties are nevertheless also due to the delocalized π-electrons that have strong correlations. Various experiments and theories show that the macroscopic nonresonant $\chi^{(3)}$ ranges from 10^{-12} to 10^{-11} esu, with corresponding molecular γ from 10^{-34} to 10^{-33} esu. These results can be unified through a semi-quantitative model[67] that applies the results from the polyene study. Larger values have also been reported, but they were either resonantly enhanced, meaning having little or no applications due to absorptive losses, or not of electronic origin.

B. Enhancement Mechanisms

Third order nonlinearities in organic materials, as described above, are currently either insufficient or barely sufficient for most device applications (see Figure 9). Attempts to increase γ in organic systems by increasing the conjugation limit have reached an upper limit. The "record" for largest γ, held jointly by poly diacetylene (PDA) and poly toluene sulfonate (PTS), is almost a decade old. Recent searches for materials with larger third

order nonlinearities have proved fruitless. In light of these results, a number of efforts have been made in fundamentally new directions to enhance γ in organic materials. These include initiation of nonlinear optical processes from excited states[68][69], investigation of the role of collective excitation in polymer systems[70], and efforts to alter the character of the ground state of conjugated molecules by changing the bond length alternation between the single and double bonds[10]. Investigations into each of these methods are currently underway.

Nonlinear optical processes from excited state populations enhance the magnitude of the nonlinearity in three ways. First, the transition frequencies between energy levels coupled to the excited state, which appear in the denominator of the perturbation expression for the susceptibility, are much smaller than those between the ground and any excited state. This is a general property of organic materials, and can be seen in the linear absorption spectrum, where there is often only one or two strong peaks. These peaks always appear in the visible or ultraviolet region, indicating that there is a "bandgap" between the ground state and the excited state manifold. Second, many more states are strongly coupled to the excited state than to the ground state. This is evident from excited state absorption measurements of organic materials, which often reveal many peaks, in contrast to the linear absorption spectrum. Third, theoretical calculations show that the degree of competition between the contribution of terms of opposite sign to the susceptibility is reduced when the processes begin in the excited state. These effects unite to result in an excited state susceptibility that can differ by orders of magnitude or even change sign from the ground state susceptibility. This enhancement mechanism can be generalized to all organic systems and all nonlinear optical processes. Experiments have confirmed the enhancement of γ by orders of magnitude due to the excited state population in organic molecules. The catch in this case is that population of the excited states must be created by optical pumping or, in some special cases, by application of an electric field.

The role of collective excitation in nonlinear optical processes which occur in polymeric systems is still not understood. Recent experiments by Japanese and US researchers have shown the existence of coherently propagating strings of excitons, which are the counterpart of excited states in molecules. Excitons consist of excited electrons and the holes left behind by the excitation process. These electron-hole pairs are bound by coulombic attractions. Strings up to three excitons long were experimentally observed. Other collective excitations, such as polarons and bipolarons, are thought to exist in organic and polymeric materials. These excitations may be exploited to increase γ in organic systems.

The role of bond length alternation (BLA) is also currently under investigation for third order processes. Researchers at Caltech have performed calculations of the third order susceptibility as a function of bond length alternation in conjugated structures. These calculations show that the systems which currently exhibit the largest γ values are not on the peak of the function. From these calculations, it is estimated that γ can be increased by up to five times by optimizing a molecules bond length alternation. A change in bond length alternation represents a change in the charge density distribution of the ground state of the molecule. An increase in bond length alternation represents an increase in the charge separation of the ground state of a molecule.

C. Photorefractive Effects

Researchers have recently begun to investigate organic materials for photorefractive nonlinear optical devices. Four step are involved in the photorefractive process. In the first step, two incident beams of light interfere within the material to create a periodic intensity distribution. The input light causes impurities or electron donating or accepting groups doped into the material to release charges. These charge carriers (in this case taken to be holes) migrate towards the dark regions of the material and become trapped. The areas from which these carriers originated then have net negative charges. This results in a

periodic charge distribution within the material. The periodic charge distribution leads to a periodic electric field. Finally, the electric field in the material alters the index of refraction periodically through the linear electro-optic effect discussed previously. The index of refraction "grating" created in this manner has many uses: it can couple two input beams of light, or link three input beams of light in a four-wave mixing scheme to produce phase conjugate waves. Research in this area originally focused on inorganic crystals, such as $BaTiO_3$. Recent research has shown that organic materials[71] can be used in photorefractive devices and illustrates the strengths that organic materials possess.

A photorefractive material must possess four properties - generation of charge carriers by input light, transport of the charge carriers, trapping of the charge carriers in the dark regions and electro-optic response - which correspond to the four steps of the photorefractive process. Organic systems in which photorefractive effects are studied typically consist of thin films of conducting polymers doped with charge donating and nonlinear optical molecules. This approach again shows the unique versatility of organic systems: the four properties needed for photorefraction can be varied almost independently by changing the backbone or the dopant molecules to produce a large variety of candidate materials. In inorganic systems, the properties of crystals cannot be changed so easily because nonlinear optical and conduction properties are intimately tied to the crystal band structure. Recently, researchers at IBM Almaden Research Center have fabricated photorefractive devices based on the charge transporting polymer poly (N-vinyl carbazole) doped with EO chromophores. These devices have shown grating diffraction efficiencies, a measure of the effectiveness of the photorefractive process in a material, and response times close to those of inorganic devices (see Figure 10). Research into organic polymer based photorefraction is still in its initial stages (the first measurement of photorefractive nonlinearities in organic polymers occurred in 1991), so vast improvements are expected.

CONCLUSION

We have reviewed the microscopic origin, features, and various applications of nonlinear optical effects in organic and polymeric materials, focusing on second- and third-order optical processes. The relatively large, ultrafast, nonresonant nonlinear optical responses of these materials lie in the correlated motion of the π electrons that are delocalized throughout the entire structures. In particular, in asymmetric structures, second-order optical effects were found to be due to the charge transfer of the π electrons from one side (usually donors) to the other (usually acceptors). The macroscopic noncentrosymmetry which are required for having bulk $\chi^{(2)}$ can be achieved through crystal growth, Langmuir-Blodgett film, and more importantly, through electric field poling. The central focus of the current research on second-order materials is toward finding structures possessing both primary large optical effects and good secondary properties such as thermal, chemical and photo stabilities and compatibility with other technologies well in semiconductor industry. The goal is to achieve applications such as high bandwidth EO modulations and efficient blue or violet light generations in integrated optical devices.

Third-order optical effects in organic materials were found to be due to electron-electron correlation effects of the delocalized π electrons. Although various structures possessing large $\chi^{(3)}$ have been found, these values are still one or two orders away from any realistic device application. Several attempts to enhance $\chi^{(3)}$ effects have been made that include excited state populations, intermolecular collective effects, and bond length alternations. The photorefractive effects, in comparison, are most promising in terms of device applications utilizing third order optical effects.

REFERENCES

1. L.A. Hornak , ed., *Polymers for Lightwave and Integrated Optics: Technology and Applications* (Marcel Dekker, New York, 1992).
2. A.F. Garito, and H. Sasabe, eds., *The Nonlinear Optics of Organic and Polymer Systems and Photonic Devices Symposium*, Nonlinear Opt. **3**, 1992.
3. M.G. Kuzyk, and J.D. Swalen, eds., *Progress in Nonlinear Optics: Organic and Polymeric Materials*, Nonlinear Opt. **6**, 1993.
4. G. R. Mohlmann, ed.,*Nonlinear Optical Properties of Organic Materials VI*, Proc. SPIE **2025**, 1993.
5. L.Y. Chiang, A.F. Garito, D. J. Sandman, eds.,*Electrical, Optical, and Magnetic Properties of Organic Solid State Materials*, Mater. Res. Soc. Proc. **247**, 1992.
6 P. N. Prasad and D.J. Williams, *Introduction to Nonlinear Optical Effects in Molecules and Polymers*, John Wiley &Sons, Inc. 1991.
7. R.F. Shi, M.H. Wu, S. Yamada, Y.M. Cai, and A.F. Garito, App. Phys. Lett. **63**. 1173(1993).
8. C.C. Teng, and A.F. Garito, Phys. Rev. B**28**, 6766(1983) and ref. therein.
9. S.R. Marder, D.N. Beratan, L.T. Cheng, Science, **252**, 103(1991).
10. S.R. Marder, J.W. Perry, G. Bourhill, C.B. Gorman, B.G. Tiemann, and K. Mansour, Science, 261, 186(1993).
11. K.D. Singer and A.F. Garito, J. Chem. Phys. **75**, 3572(1981).
12. F. Kajzar, and J. Messier, Phys. Rev. A**32**, 2352(1985).
13. see for example, M. A. Mitchell, M. Tomida, A.B. Padias, H.K. Hall, H.S. Lackritz, D.R. Robello, C.S. Robello, C.S. Willand, and D.J. Williams, Chem. Mater. **5**, 1044(1993).
14. K. Clays and A. Persoons, Phys. Rev. Lett. **66**, 2980(1991).

15. W.M. Laidlaw, R.G. Denning, T. Verbiest, E. Chauchard, and A. Persoons, Nature **363**, 58(1993).

16. T. Verbiest, K. Clays, A. Persoons, F. Meyers, and J.L. Bredas, Opt. Lett. **18**, 525(1993).

17. J. Zyss, J. Chem. Phys. **98**, 6583(1993).

18. K. Clays, E. Hendrickx, M. Triest, T. Verbiest, C. Dehu, and J.L. Bredas, Science **262**, 1419(1993).

19. T. Matsuura, S. Ando, S. Matsui, H. Hirata, S. Sasaki, and F. Yamamoto, in *Organic Thin Films for Photonic Applications Technical Digest*, 1993, Vol **17**, (Optical Society of America, Washington, DC, 1993), pp262.

20. G. Khanarian, M.A. Mortazavi, and A.J. East, App. Phys. Lett. **63**, 1462(1993).

21. T.F. Heinz, H.W.K. Tom, and Y.R. Shen, Phys. Rev. A**28**, 1883(1983).

22. G.T. Boyd, Y.R. Shen, and T.W. Haensch, Opt. Lett. **11**, 97(1986).

23. C.T. Seto, and G.M. Whitesides, J. Am. Chem. Soc. **115**, 905(1993).

24. D.R. Dai, T.J. Marks, J. Yang, P.M. Lundquist, and G.K. Wong, Macromolecules **23**, 1894(1990).

25. S. Yitzchaik, S.B. Roscoe, A.K. Kakkar, D.S. Allan, T.J. Marks, Z.Y. Xu, T.G. Zhang, W.P. Lin, and G.K. Wong, J. Phys. Chem. **97**, 6958(1993).

26. K.D. Singer, J.E. Sohn, and S.J. Lalama, App. Phys. Lett. **49**, 248(1986).

27. K.D. Singer, M.G. Kuzyk, and J.E. Sohn, J. Opt. Am. Soc. **B4**, 968(1987).

28. P. A. Cahill, K.D. Singer, and L.A. King, Opt. Lett. **14**, 1137(1989).

29. H.L. Hampsch, J.M. Torkelson, S.J. Bethke, and S.G. Grubb, **67**, 1037(1990).

30. J. Wu, J.F. Valley, S. Ermer, E.S. Binkley, J.T. Kenney, G.F. Lipscomb, and R. Lytel, App. Phys. Lett. **58**, 225(1991).

31. Y. Shi, W.H. Steier, M. Chen, L.P. Yu, and L.R. Dalton, App. Phys. Lett. **60**, 2577(1992).

32. P.M. Radom, Y.Shi, W.H. Steier, C.Z. Xu, B. Wu, and L.R. Dalton, App. Phys. Lett. **62**, 2605(1993).

33. X.F. Cao, J.P. Jiang, D.P. Bloch, R.W. Hellwarth, L.P. Yu, and L.R. Dalton, J. App. Phys. **65**, 5012(1989).

34. P.A. Cahill, C. H. Seager, M. B. Meihhardt, A. J. Beuhler, D.A. Wargoeski, K.D. Singer, T.C. Kowalczy, and T.Z. Kosc, Proc. **2025**, 48(1993).

35. J.W. Wu, E.S. Binkley, J.T. Kenney, R. Lytel, and A.F. Garito, J. Appl. Phys. **69**, 7366(1991).

36. M. Staehelin, D.M. Burland, M. Ebert, R.D. Miller, B.A. Smith, R.J. Twieg, W. Volksen, and C.A. Walsh, App. Phys. Lett. **61**, 1626(1992).

37. V.P. Rao, A.K.Y. Jen, K.Y. Wong, K.J. Drost, J. Am. Chem. Soc. **14**, 1118(1993).

38. J.I. Thackara, G.F. Lipscomb, M.A. Stiller, A.J. Ticknor, and R. Lytel, App. Phys. Lett. **52,** 1031(1988).

39. K. Sasaki, Y. Nonaka, T. Kinoshita, E. Nihei, and A. Koike, Nonliner Opt. **3**, 61(1992).

40. C.C. Teng, App. Phys. Lett. **60**, 1538(1992).

41. A.F. Garito and K.D. Singer, Laser Focus **18**, 59(1982).

42. A. Harada, Y. Okazaki, K. Kamiyama, and S. Umegaki, App. Phys. Lett. **59**, 1535(1991).

43. G. Khanarian, M.A. Mortazavi, and A.J. Eat, App. Phys. Lett. **63**, 1462(1993).

44. T.L. Penner, H.R. Motschmann, N.J. Armstrong, M.C. Ezenyilimba, D.J. Williams, Nature **367**, 49(1994).

45. H.S. Nalwa, T. Watanabe, A. Kakuta, A. Mukoh, and S. Miyata, App. Phys. Lett. **62**, 3223(1993).

46. J.L. Bredas, C. Adant, P. Tackx, A. Persoons, and B.M. Pierce, Chem. Rev. (in press).

47. A. M. Weiner, S. De Silverstri, and E.P. Ippen, J. Opt. Am. Soc. **B2**, 654(1985).

48 T. Kobayashi, M. Yoshizawa, M. Taiji, and Hasegawa, J. Opt. Soc. Am. **B7**, 1558(1990).

49. J.R. Heflin, K.Y. Wong, O. Zamani-Khamiri, and A.F. Garito, Phys. Rev. B**38**, 1573(1988).

50. J. W. Wu, J. R. Heflin, R. A. Norwood, K. Y. Wong, O. Zamani-Khamiri, A.F. Garito, P. Kalyanaraman, and J. Sounik, J. Opt. Soc. Am. **B6**, 707 (1989).

51. B.M. Pierce, J. Chem. Phys. **91**, 791(1989).

52. Z.G. Soos and S. Ramasesha, J. Chem. Phys. **90**, 1067(1989).

53. S.N. Dixit, D. Guo, S. Mazumdar, Phys. Rev. **B43**, 6781(1991).

54. S. Mukamel and H.X. Wang, Phys. Rev. Lett. **192**, 417(1992).

55. C.W. Dirk, L-T. Cheng, and M.G. Kuzyk, Int. J. Quant. Chem. **43**, 27(1992).

56. Q.L. Zhou, R.F. Shi, O. Zamani-Khamiri, and A.F. Garito, Nonliear Opt. **6**, 145(1993).

57. M. Hosoda, T. Wada, A. Yamada, A.F. Garito, and H. Sasabe, Jpn, J. App. Phys. **30**, L1486(1991).

58. B.A. Reinhardt, M.R. Unroe, R.C. Evers, M. Zhao, M. Samoc, P.N. Prssad, and M. Sinsky, Chem. Mater. **3**, 864(1991).

59. H. Vanherzeele, J. S. Meth, S.A. Jenekhe, and M. F. Roberts, J. Opt. Soc. Am. **B9**, 524(1992).

60. K. Ichimura, H. Matsuda, H. Nakanishi, T. Kobayashi, Phys. Rev. B**47**, 6250(1993).

61. D. Guo, S. Mazumdar, G.I. Stegeman, M. Cha, D. Neher, S. Aramaki, W. Torruellas, R. Zanomi, in ref. 2, pp151.

62. Q.L. Zhou, Ph.D. Dissertation, University of Pennsylvania, Philadelphia, PA (1993).

63. H. Thienpont, G.L.J.A. Rikken, E.W. Meijer, Phys. Rev. Lett. **65**, 2141(1990).

64. S.A. Jenekhe, W.C. Chen, S. Lo, and S.R. Flom, App. Phys. Lett. **57**, 126(1990).

65. Z.H. Kafafi, J.R. Lindle, R.G.S. Pong, F.J. Bartoli, L.J. Lingg, and J. Milliken, Chem. Phys. Lett. **188**, 492(1992).

66. F. Kajzar, C. Taliani, R. Zamboni, S. Rossini, and R. Danieli, in ref. 4, pp352 and the references therein.

67. A.F. Garito, R.F. Shi, J.R. Heflin, R. Lytel, G.F. Lipscomb, and A.J. Ticknor, in *Spatial Light Modulators: Materials, Devices, and Applications*, U. Efron, Ed. Marcel Dekker, Inc, (in press).

68. Q.L. Zhou, J.R. Heflin, K.Y. Wong, O. Zamani-Khamiri, and A.F. Garito, Phys. Rev. **A43**, 1673(1991).

69. D.C. Rodenberger, J.R. Heflin, and A.F. Garito, Nature **359**, 309(1992).

70. M Kuwata-Gonokami, N. Peyghambarian, K. Meissner, B. Fluegel, Y. Sata, K. Ema, R. Shimano, S. Mazumdar, F. Guo, T. Tokihiro, H. Ezaki, and E. Hanamura, Nature, **367**, 47(1994).

71. S. Ducharme, J.C. Scott, R.J. Twieg, and W.E. Moerner, Phys. Rev. Lett. **66**, 1846(1991).

Figure Captions:

Figure 1. Top two: Schematic molecular structure of 1,8-naphthoylene-(3'-amino) benzimidazole-4,5-dicarbox-N-(2,5-di-tert-butyl) phenylimide and its electron charge density distribution difference contour diagram between the first excited and ground states. Bottom three: Schematic molecular structure of all *trans*-hexatriene and its electron transition density matrix contour diagrams between the 1^1B_u and 1^1A_g states and between the 1^1B_u and ground 1^1A_g states, respectively. In these contour diagrams, regions with solid and dashed curves indicate increased and decreased electron density, respectively.

Figure 2. Examples of structures of NLO side-chain polymers for electric field poling. (a) Backbone: acrylate, spacer: C6 aliphatic chain, NLO side group: 4-methoxy-4'-nitrostilbene (MONS). (b) Backbone: acrylate, spacer: 6-ring: NLO side group: 4-dimethylamino-4'-nitrostilbene (DANS). (Ref. R. Norwood of Hoechst Celanese).

Figure 3. Comparative figures of merit for polymers, lithium niobate ($LiNbO_3$) and gallium arsenide (GaAs).

Figure 4. Polyimide rib waveguide structure for a perfect shuffle data processing function (Ref. B. Booth of Dupont and A. Husain, formerly of Honeywell).

Figure 5. Dispersion of SHG d_{11} of MNA as a function of fundamental photon energy

Figure 6. Spectral dispersion of the magnitude (a) and phase (b) of the third order coefficient $\chi^{(3)}(-3\omega; \omega,\omega,\omega)$ of poly-4BCMU. Data are experimental and solid curves are from theoretical calculations that explicitly account for electron correlations (Ref. G. Stegeman of University of Central Florida, CREOL).

Figure 7. Calculated log-log plot of isotropically averaged $\langle\gamma(-3\omega; \omega,\omega,\omega)\rangle$ at $h\omega$=0.65 eV versus the number of sites and correlation length for *trans*, *cis*, and *cyclic* polyenes. The three polyene series follow the same length dependence of $\langle\gamma(-3\omega; \omega,\omega,\omega)\rangle \propto L^{3.5}$

Figure 8. Molecular third order optical coefficient $\gamma(-2\omega; \omega,\omega,0)$ versus the number of repeat units for oligothiophenes in a PMMA matrix at room temperature. The solid line in only meant to guide the eye

Figure 9. Possible application areas for third order nonlinear optical polymers (Ref. T. Kaino of Nippon Telephone and Telegraph (NTT)).

Figure 10. Comparison inorganic and polymer photorefractive materials. Saturation diffraction efficiency η_{ss} versus growth rate τ^{-1}, scaling to 1 mm thickness and assuming 1 W/cm^2 writing intensity (Ref.W.E. Moerner of IBM Almeden).

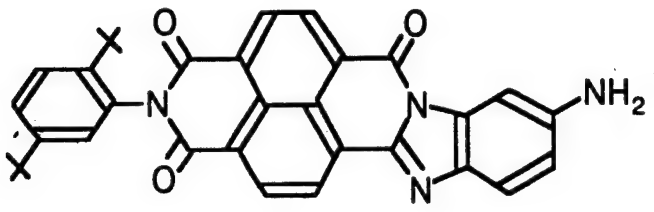

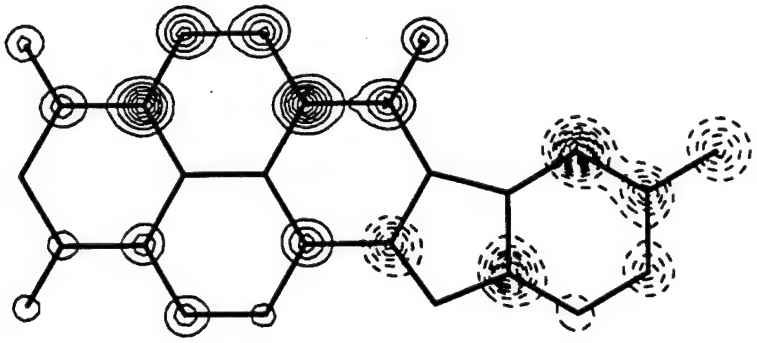

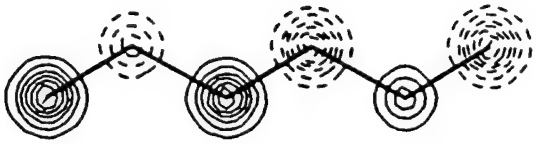

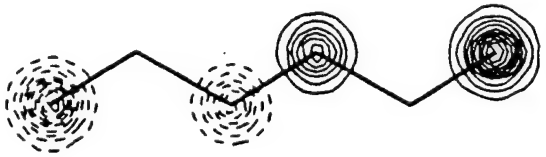

Fig. 1

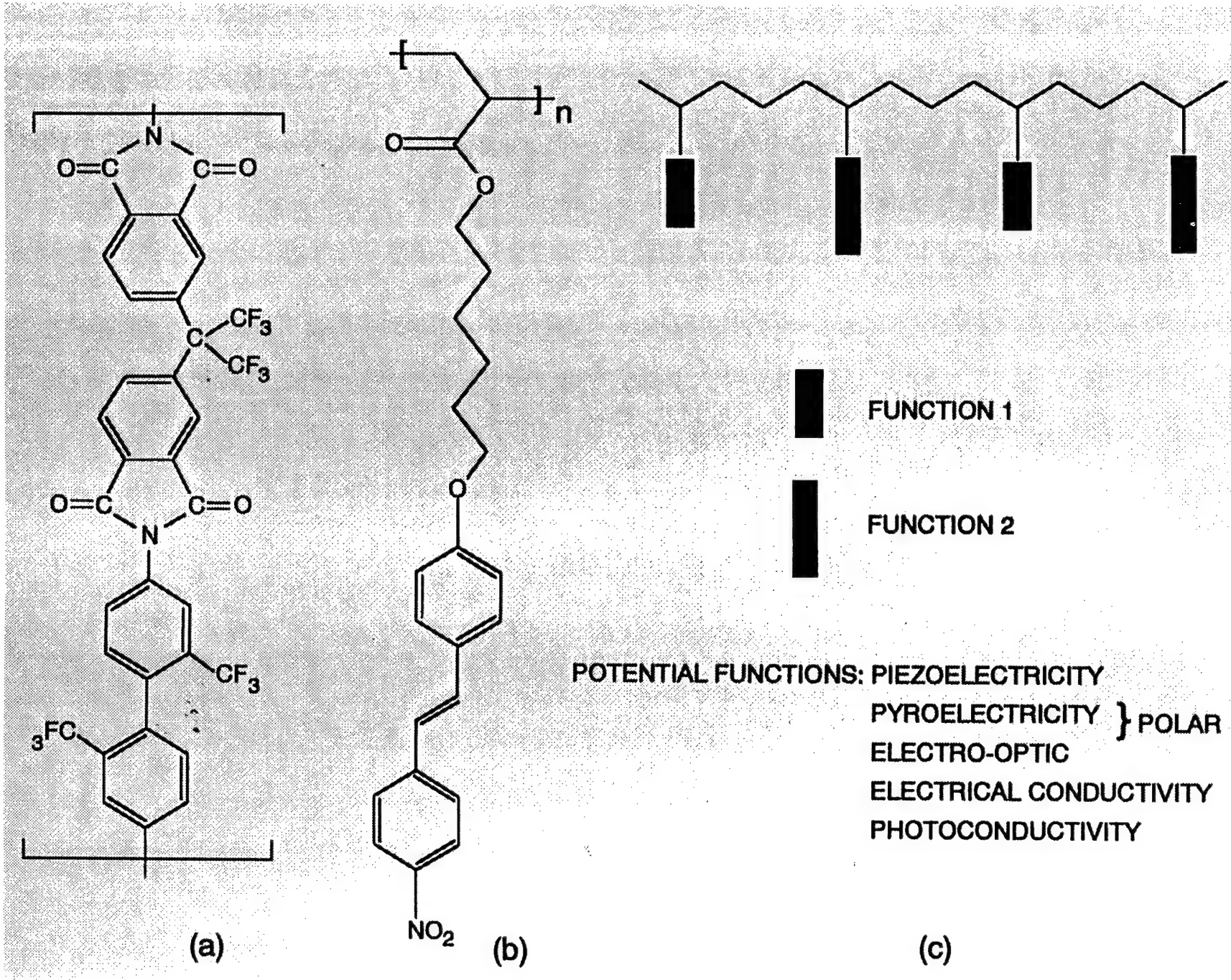
(a)
(b)
(c)
FUNCTION 1
FUNCTION 2
POTENTIAL FUNCTIONS: PIEZOELECTRICITY
PYROELECTRICITY } POLAR
ELECTRO-OPTIC
ELECTRICAL CONDUCTIVITY
PHOTOCONDUCTIVITY

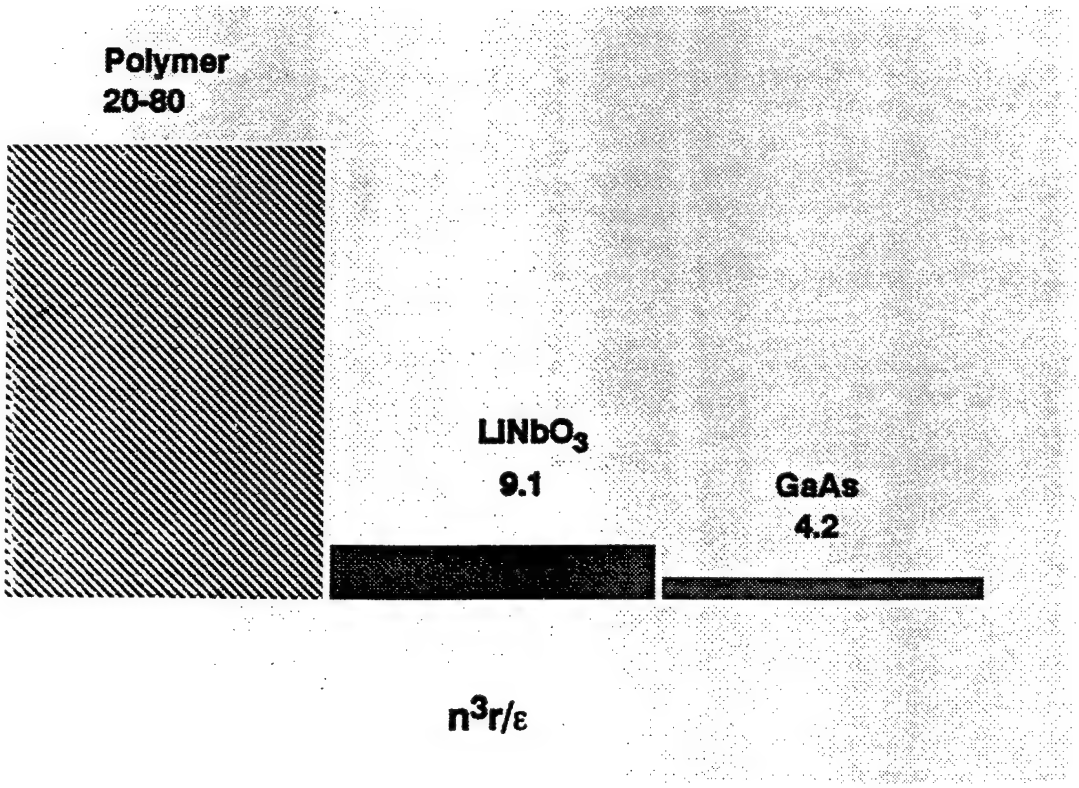

Fig. 3

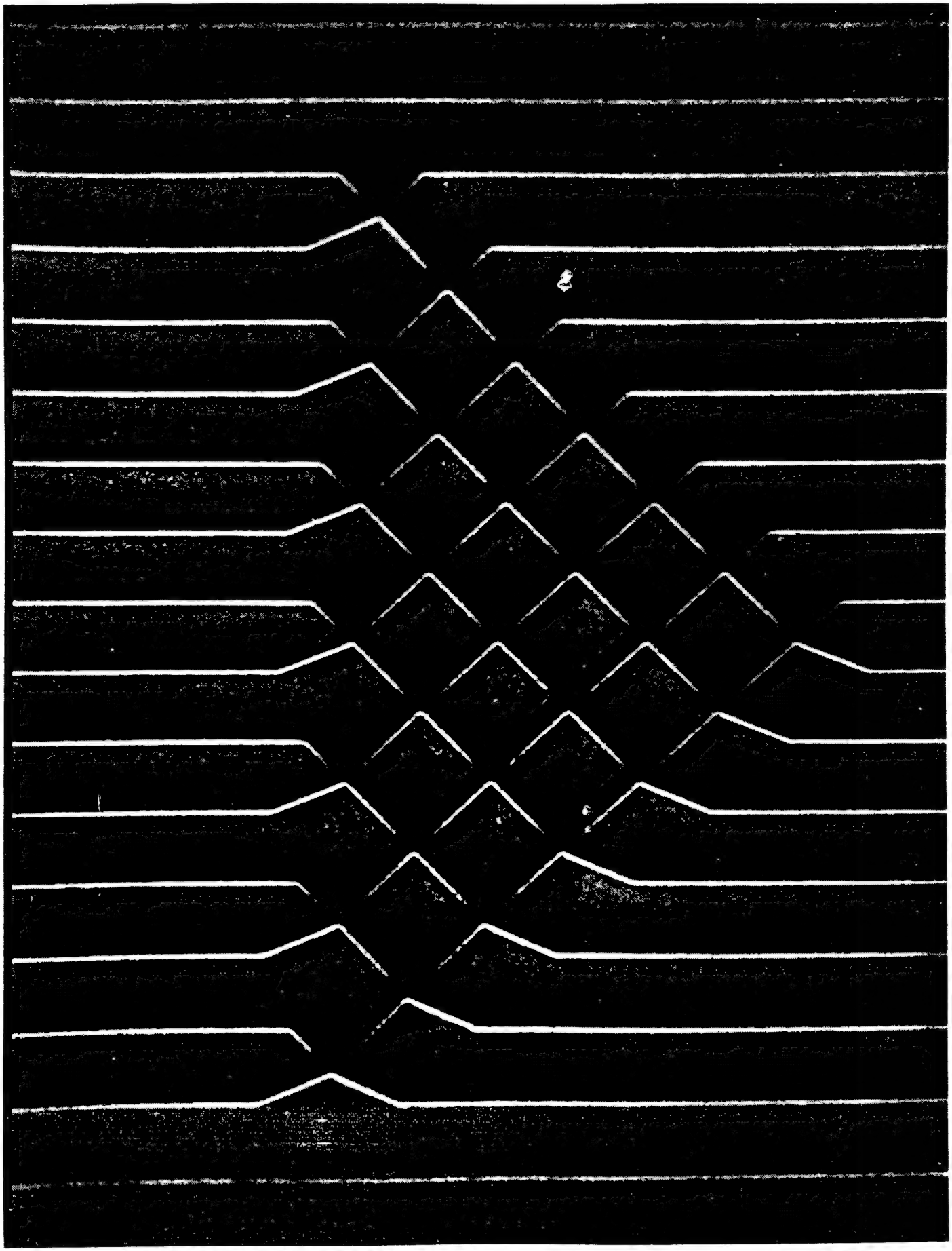

Fig. 4

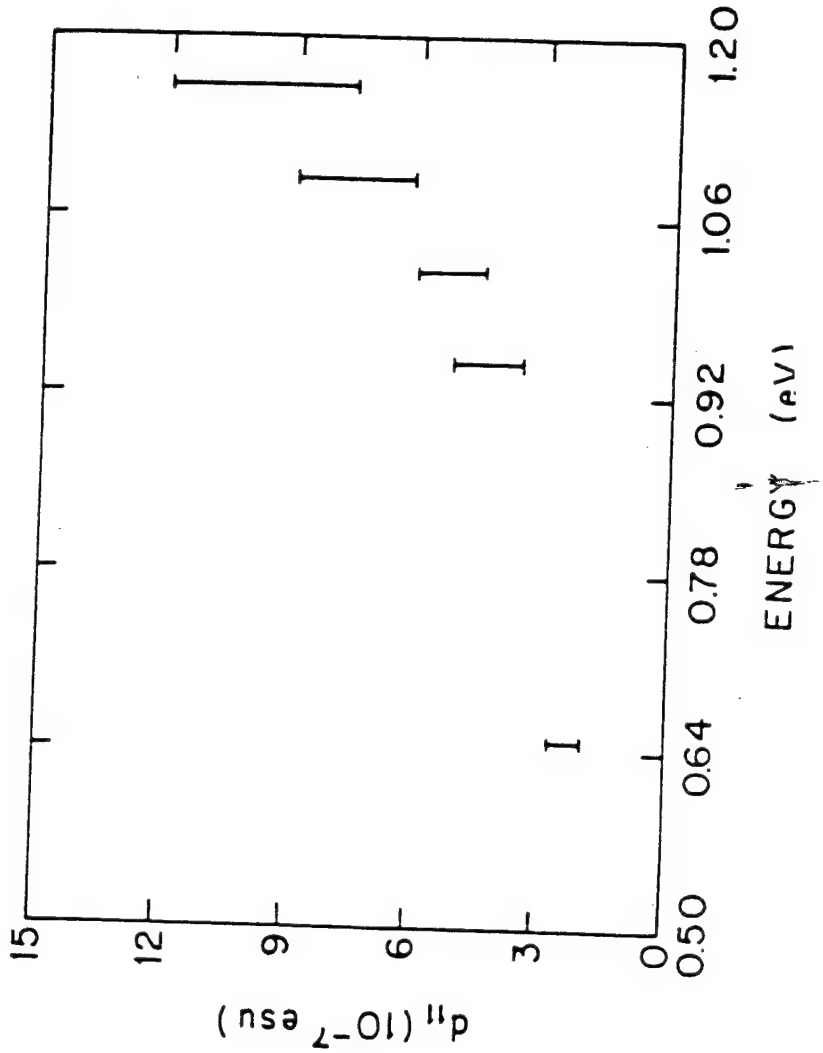

Figure

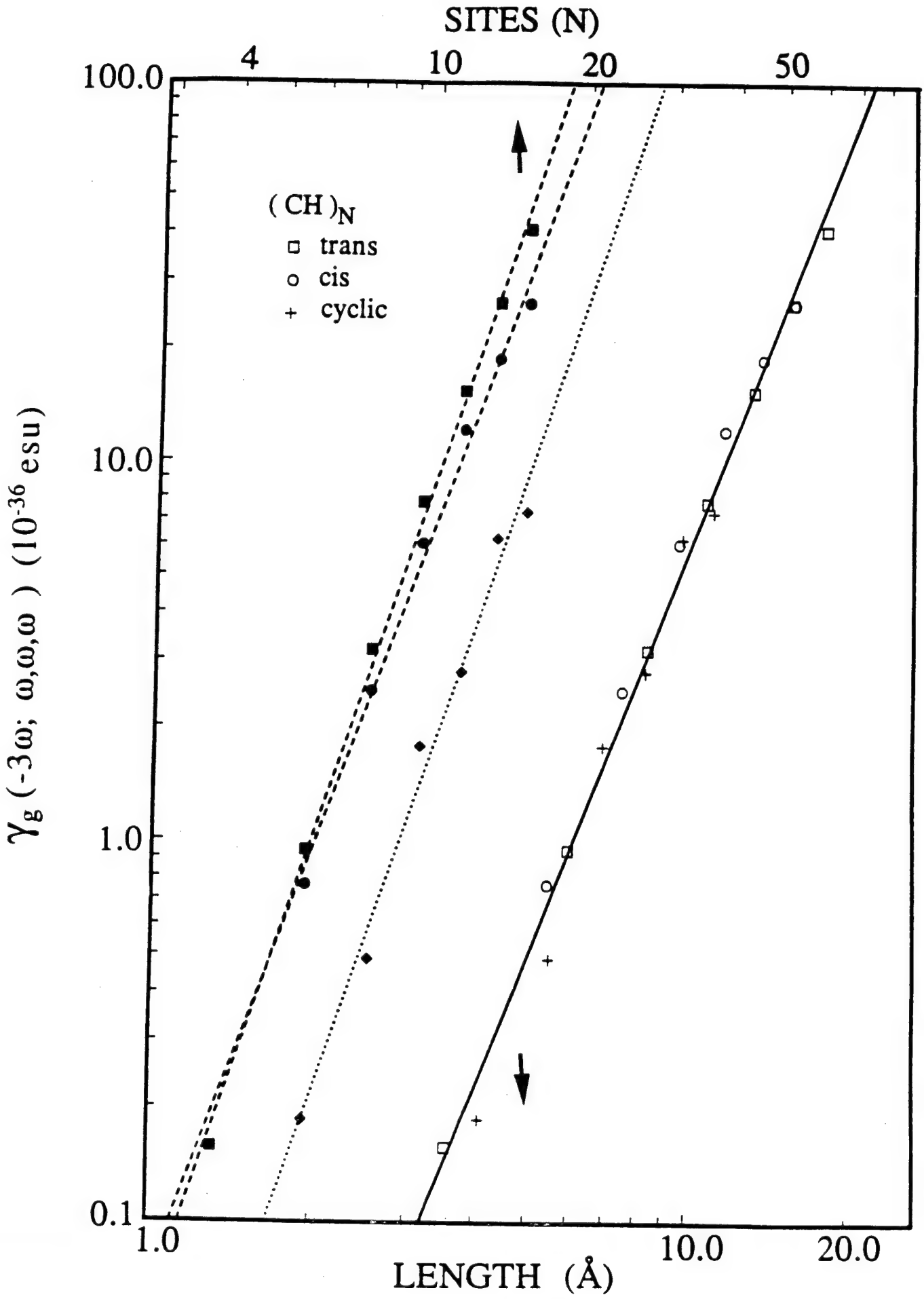
SITES (N)
4
10
20
50
100.0
10.0
1.0
0.1
γ_g (-3ω; ω,ω,ω) (10^{-36} esu)
(CH)$_N$
trans
cis
cyclic
1.0
10.0
20.0
LENGTH (Å)

Fig. 6

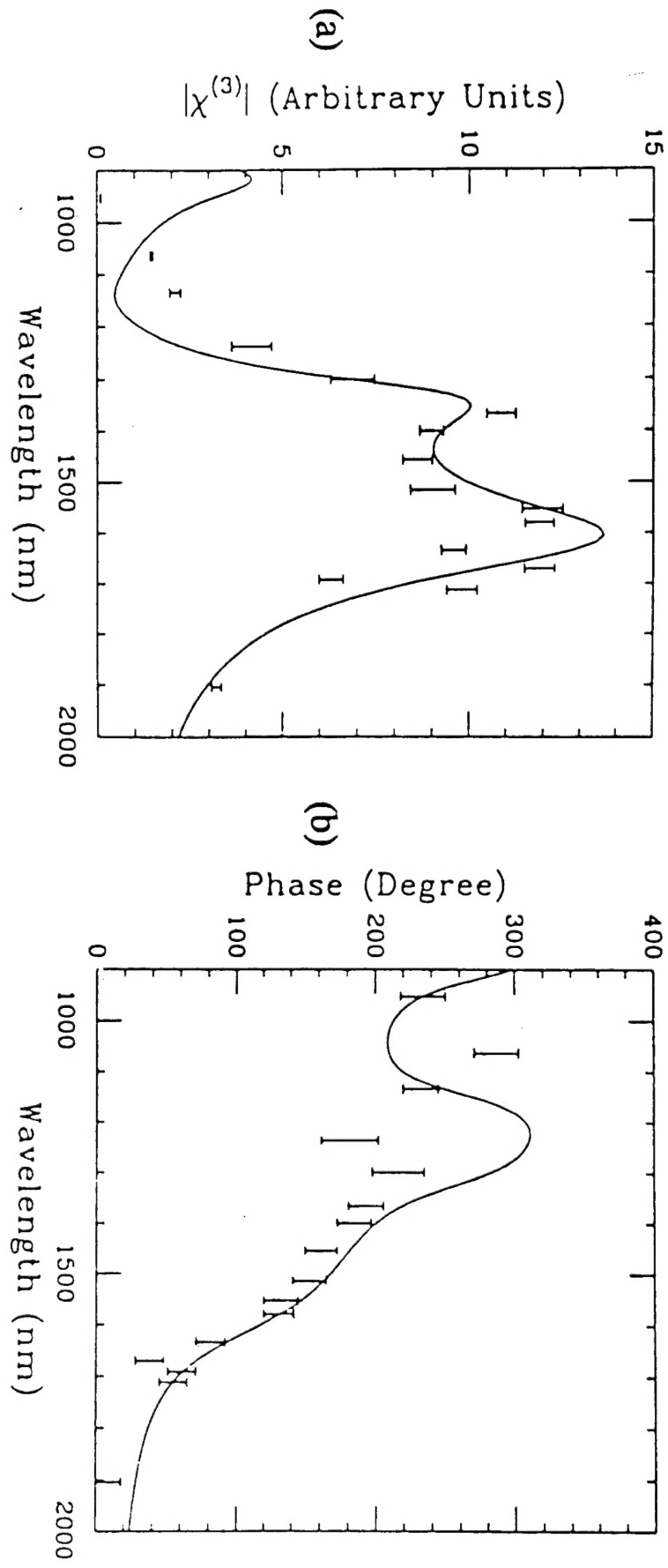
(a)
$|\chi^{(3)}|$ (Arbitrary Units)
0
5
10
15
1000
1500
2000
Wavelength (nm)
(b)
Phase (Degree)
0
100
200
300
400
1000
1500
2000
Wavelength (nm)

Fig. 7

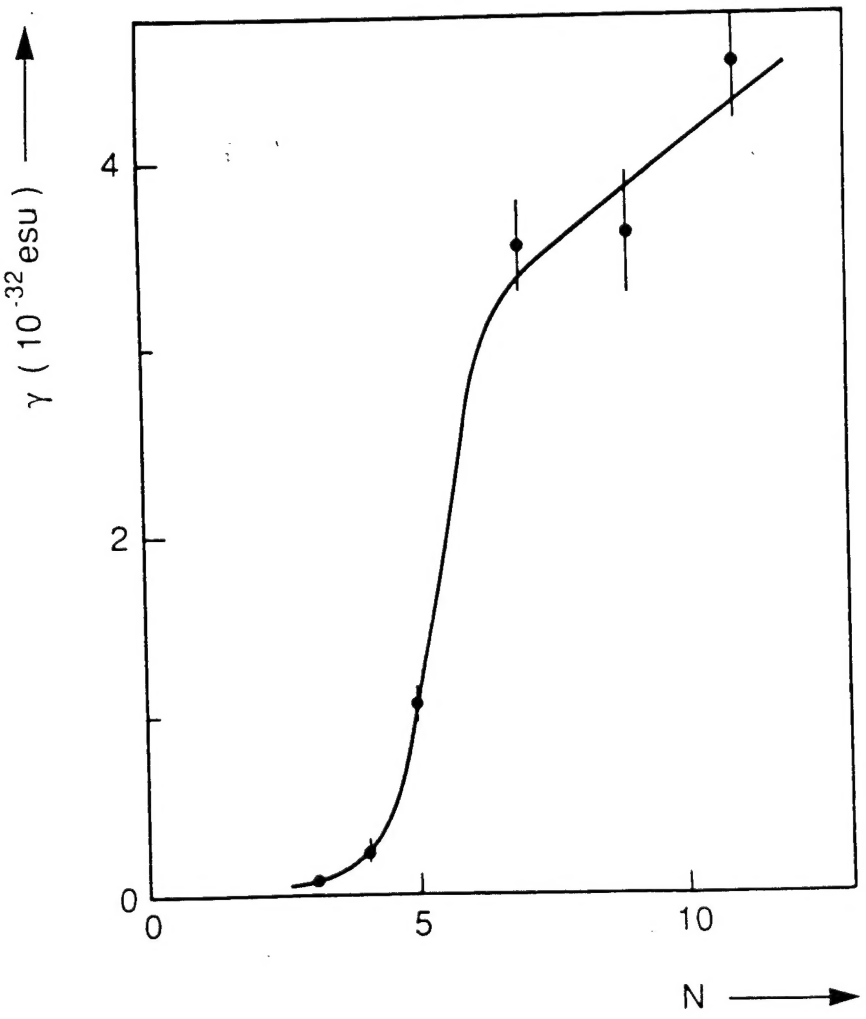

Fig. 8

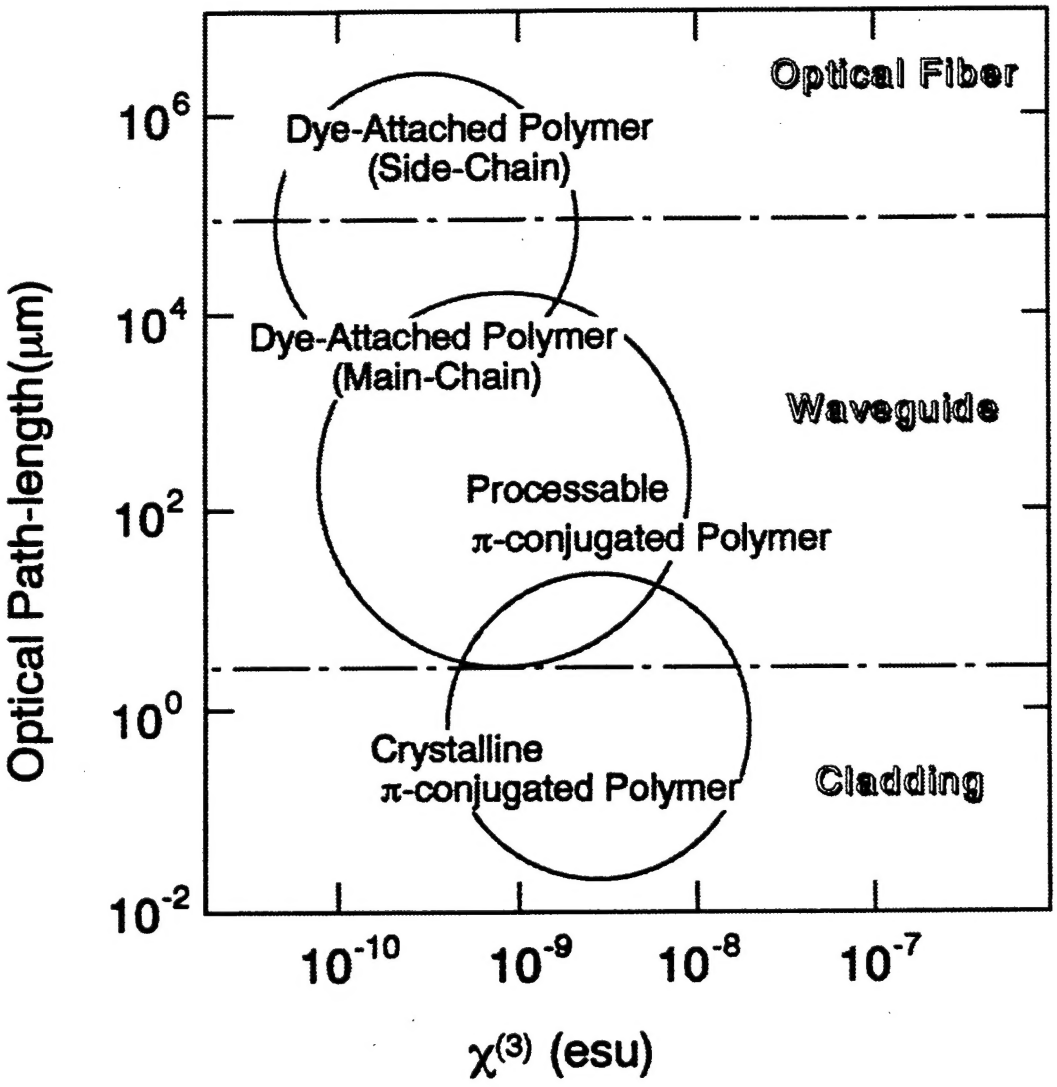
Optical Fiber
Dye-Attached Polymer
(Side-Chain)
Dye-Attached Polymer
(Main-Chain)
Waveguide
Processable
π-conjugated Polymer
Crystalline
π-conjugated Polymer
Cladding
Optical Path-length(μm)
10^6
10^4
10^2
10^0
10^-2
10^-10
10^-9
10^-8
10^-7
χ(3) (esu)

Fig. 9

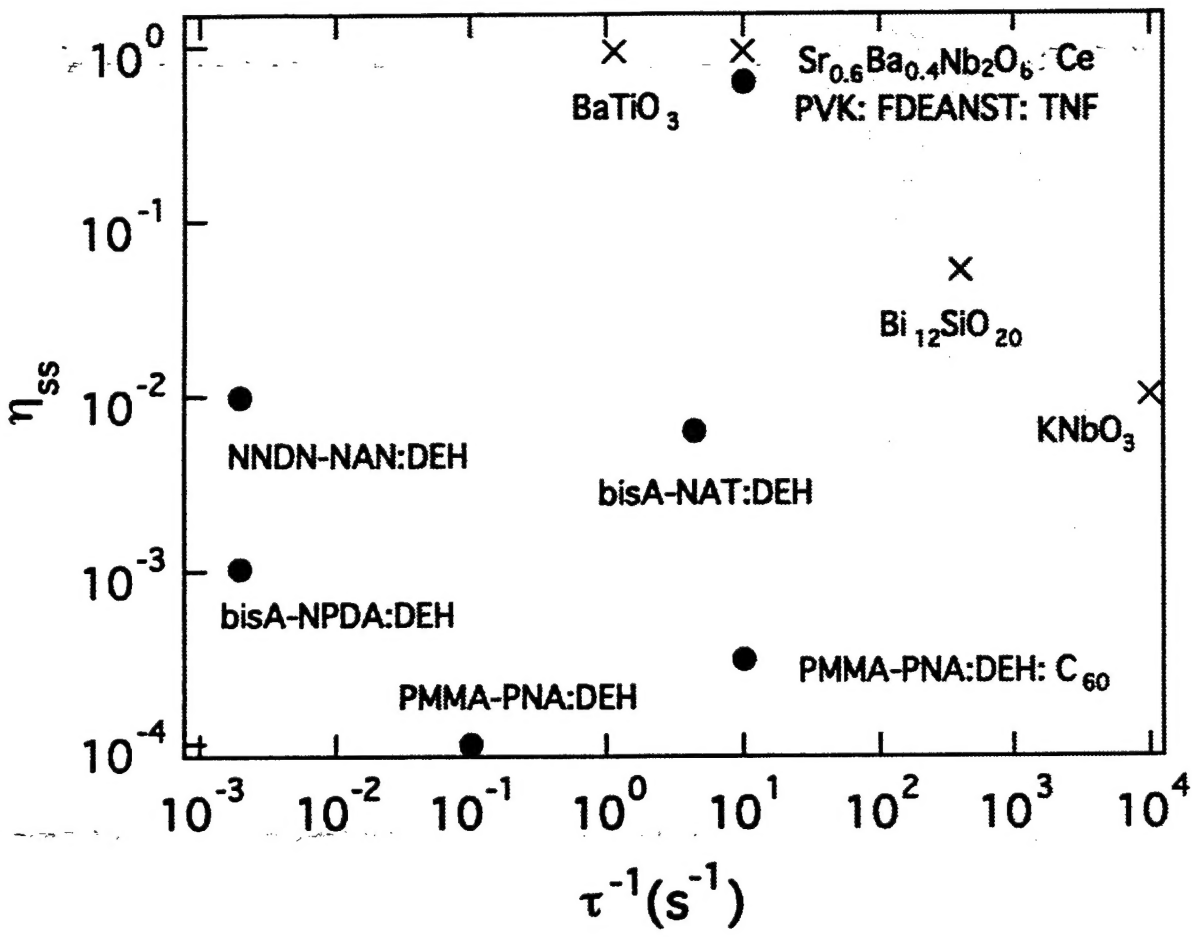
10^0
10^{-1}
10^{-2}
10^{-3}
10^{-4}
η_{ss}
10^{-3} 10^{-2} 10^{-1} 10^0 10^1 10^2 10^3 10^4
$\tau^{-1}(s^{-1})$
$BaTiO_3$
$Sr_{0.6}Ba_{0.4}Nb_2O_6$: Ce
PVK: FDEANST: TNF
$Bi_{12}SiO_{20}$
$KNbO_3$
NNDN-NAN:DEH
bisA-NAT:DEH
bisA-NPDA:DEH
PMMA-PNA:DEH
PMMA-PNA:DEH: C_{60}

Fig. 10